Conserved Amino Acids within the Adenovirus 2 E3/19K Protein Differentially Affect Downregulation of MHC Class I and MICA/B Proteins

Martina Sester,*,† Katja Koebernick,*,[1] Douglas Owen,*,[2] Minghui Ao,*,[2] Yana Bromberg,‡ Ed May,* Emily Stock,* Lawrence Andrews,* Veronika Groh,§ Thomas Spies,§ Alexander Steinle,¶ Beatrice Menz,*,[3] and Hans-Gerhard Burgert*

Successful establishment and persistence of adenovirus (Ad) infections are facilitated by immunosubversive functions encoded in the early transcription unit 3 (E3). The E3/19K protein has a dual role, preventing cell surface transport of MHC class I/HLA class I (MHC-I/HLA-I) Ags and the MHC-I–like molecules (MHC-I chain-related chain A and B [MICA/B]), thereby inhibiting both recognition by CD8 T cells and NK cells. Although some crucial functional elements in E3/19K have been identified, a systematic analysis of the functional importance of individual amino acids is missing. We now have substituted alanine for each of 21 aas in the luminal domain of Ad2 E3/19K conserved among Ads and investigated the effects on HLA-I downregulation by coimmunoprecipitation, pulse-chase analysis, and/or flow cytometry. Potential structural alterations were monitored using conformation-dependent E3/19K-specific mAbs. The results revealed that only a small number of mutations abrogated HLA-I complex formation (e.g., substitutions W52, M87, and W96). Mutants M87 and W96 were particularly interesting as they exhibited only minimal structural changes suggesting that these amino acids make direct contacts with HLA-I. The considerable number of substitutions with little functional defects implied that E3/19K may have additional cellular target molecules. Indeed, when assessing MICA/B cell-surface expression we found that mutation of T14 and M82 selectively compromised MICA/B downregulation with essentially no effect on HLA-I modulation. In general, downregulation of HLA-I was more severely affected than that of MICA/B; for example, substitutions W52, M87, and W96 essentially abrogated HLA-I modulation while largely retaining the ability to sequester MICA/B. Thus, distinct conserved amino acids seem preferentially important for a particular functional activity of E3/19K. ***The Journal of Immunology*****, 2010, 184: 255–267.**

Human adenoviruses (Ads) can cause diseases of the eyes, respiratory tract, and the gastrointestinal tract (1). More than 50 different Ad serotypes have been distinguished, which are classified in six different species (2). In a considerable proportion of patients, Ads persist for a variable length of time after primary infection and may become latent (3, 4), with members of species C (e.g., Ad2 or Ad5) being most often detected (3). Their successful propagation in vivo is facilitated by multiple strategies to evade the host immune response (1, 5, 6). Many of these immune evasion functions are encoded in the early transcription unit 3 (E3), which is not required for virus replication in tissue culture cells but is preserved in all human Ads (5, 7). This suggests that E3 proteins have an important function in vivo. Indeed, over the past 2 decades, experiments both in cell culture and animal models clearly demonstrated that most E3 proteins have the capacity to modulate immune response mechanisms (5, 7–13), ranging from inhibition of Ag presentation (14), suppression of NK cell activation (15), downregulation of apoptosis receptors (7–9, 16), and interference with TNF receptor-induced activities (10, 17, 18).

The most abundant E3 protein in the early phase of the infection cycle of species C Ads is E3/19K. E3/19K functions to counter the recognition of infected cells by both innate and adaptive cellular immune responses. Recognition of cells by cytotoxic CD8 T cells is suppressed by preventing the transport of MHC class I (MHC-I) molecules (in human: HLA class I [HLA-I]) to the cell surface (19–25). More recently, we showed that E3/19K has a second function, namely, to inhibit recognition by NK cells via intracellular sequestration of the stress-induced MHC-I chain-related protein A and B (MICA/B) molecules (15), which serve as ligands for the activating NK receptor NKG2D (26, 27). Deletion of E3/19K, as found in most Ad gene therapy vectors, makes transduced or infected cells susceptible to NK cells (15, 28). As the NKG2D receptor is also expressed on human CD8 T cells, γ/δ T cells, and NKT cells, E3/19K may have a much wider immune evasion function than initially anticipated.

*Department of Biological Sciences, University of Warwick, Coventry, United Kingdom; †Department of Transplant and Infection Immunology, Institute of Virology, University of the Saarland, Homburg, Germany; ‡Center for Computational Biology, Columbia University, New York, NY 10032; §Fred Hutchinson Cancer Research Center, Clinical Research Division, Seattle, WA 98109; and ¶Department of Immunology, Institute for Cell Biology, Eberhard Karls University of Tübingen, Tübingen, Germany

[1]Current address: Institute for Biochemistry, Department of Developmental Biochemistry, University of Göttingen, Göttingen, Germany.

[2]D.O. and M.A. contributed equally to this work.

[3]Current address: Birkhäuser Verlag AG, Basel, Switzerland.

Received for publication July 21, 2009. Accepted for publication October 30, 2009.

This work was supported by SFB388 from the Deutsche Forschungsgemeinschaft and Warwick University to H.G.B. Y.B. was funded by the National Library of Medicine.

Address correspondence and reprint requests to Dr. Hans-Gerhard Burgert, Department of Biological Sciences, University of Warwick, Coventry, CV4 7AL, UK. E-mail address: H-G.Burgert@warwick.ac.uk

The online version of this article contains supplemental material.

Abbreviations used in this paper: Ad, adenovirus; β_2-m, β_2-microglobulin; C, C terminus; E3, early transcription unit 3; endo H, endoglycosidase H; ER, endoplasmic reticulum; HLA-I, HLA class I; MHC-I, MHC class I; MICA/B, MHC class I chain-related protein A and B; N, N terminus; RI, reliability index; SNAP, screening for nonacceptable polymorphisms; TM, transmembrane domain; Wt, wild-type.

www.jimmunol.org/cgi/doi/10.4049/jimmunol.0902343

The mechanism by which E3/19K prevents cell surface transport of HLA-I molecules has been established in principle (7, 19, 29). Like MHC-I, E3/19K is a type I transmembrane glycoprotein. Efficient suppression of MHC-I cell surface expression requires the combined activity of two functional entities in E3/19K: the ability of the luminal domain to bind newly synthesized HLA-I molecules, and signals in the transmembrane and/or cytoplasmic domain for localization in the endoplasmic reticulum (ER) (19, 21, 30, 31). Although the precise requirements for E3/19K-MHC-I interaction are ill-defined, ER localization is promoted by a dilysine type ER retrieval signal in the cytoplasmic tail of E3/19K molecules (31–34) that is recognized by the COPI coat, thereby mediating retrograde transport of E3/19K and associated MHC-I from the *cis*-Golgi to the ER (35). E3/19K may also be able to indirectly inhibit transport of MHC alleles by binding to the TAP and preventing efficient peptide loading (36).

E3/19K forms physical complexes with the heavy chain of most MHC-I alleles soon after translocation into the ER. This interaction is noncovalent, is independent on glycosylation of either MHC-I or E3/19K, and does not require the association of MHC-I with β_2-microglobulin (β_2-m) or peptide (37, 38). The latter is consistent with the ability of E3/19K to bind MICA/B, MHC-I–like molecules that do not associate with β_2-m or peptide (15). However, formation of the MHC-I/E3/19K complex does not prevent the subsequent assembly with peptide/β_2-m in cells or in vitro [(7, 21, 38), H.-G. Burgert, unpublished]. Rather, peptide binding and complete folding of the polymorphic peptide-binding domains α1 and α2 may facilitate the association with E3/19K (39). As a matter of fact, complex formation with E3/19K critically depends on the α1 and α2 domains of MHC-I molecules (40–43) and a number of amino acids in α1/α2 have been identified that have a profound impact on the interaction (42, 44, 45).

Ad2 and Ad5 E3/19K proteins bind the great majority of human HLA-A/B alleles, albeit with different affinities (14, 41, 44, 46), and certain MHC-I alleles of other species (23, 40, 42, 47, 48). Based on this promiscuous binding activity of E3/19K to MHC-I and MICA/B alleles, the critical target structure of HLA-I is thought to be rather conserved (42). However, all attempts to determine the three-dimensional structure of the E3/19K-MHC-I complex have not been successful as yet (38, 49).

Although the interaction does not require the cytoplasmic tail of E3/19K (21, 50, 51), the transmembrane segment might be critical for HLA-I interaction in vivo within the cell but is not essential in vitro (38, 51, 52). Hence, the interaction is primarily mediated by the luminal portion of E3/19K (30, 38, 51, 53). This suspicion was confirmed by the complete loss of HLA-I binding upon disruption in the luminal domain of the two intramolecular disulfide bonds (30) and by construction of in-frame deletions (53). However, as these mutations were associated with profound structural alterations, the functional contributions of individual amino acids remain largely unknown.

E3/19K-like glycoproteins are expressed by human Ad species B–E. Despite their common function to inhibit HLA-I transport E3/19K proteins from different Ad species display poor sequence homology (5, 10, 54–56). Only 20 of the 139–151 aas present in E3/19K homologs of different serotypes are universally conserved (Fig. 1) (5). We reasoned that the highly conserved amino acids are essential for the function and/or structural integrity of E3/19K. This hypothesis is supported by our previous observation that four conserved cysteines forming two intramolecular disulfide bonds between cysteines 11/28 and 22/83 of Ad2 E3/19K, respectively, were absolutely required for functional activity, whereas mutation of three nonconserved cysteines had no significant effect on E3/19K function (15, 30). To further examine the role of conserved residues in the ER-luminal domain of Ad2 E3/19K, we have systematically replaced all 16 strictly conserved and 5 highly conserved residues by alanines using site-directed mutagenesis. Initially, mutants were screened for their ability to form complexes with HLA-I by transient transfection into 293 cells, followed by immunoprecipitation. Mutants with a strong reduction in HLA-I binding were comprehensively characterized in permanent cell lines for their efficiency of complex formation with HLA-I, their capability to inhibit HLA-I transport, and their effect on steady-state expression of HLA-I and MICA/B at the cell surface. Interestingly, a differential effect of these mutations on HLA-I specific E3/19K functions was observed, with some mutations abrogating functional activity, whereas others caused only minor changes. Some of these latter amino acids turn out to be critical for MICA/B downregulation. Overall, many mutations have a differential impact on HLA-I and MICA/B binding. By relating the functional data to the structural changes as detected by conformation-dependent mAbs (57) amino acids were identified that may form part of the E3/19K interface binding HLA-I. In addition, a computational method (screening for nonacceptable polymorphisms [SNAP]) was used to predict the functional importance of each amino acid in the E3/19K luminal domain (58, 59).

Materials and Methods

Construction of mutant E3/19K genes

Using PCR-mediated oligonucleotide-directed mutagenesis, single amino acid codons corresponding to the amino acid positions E5, P9, T14, I26, K27, I37, K42, W52, P54, G55, Y60, V62, V64, F77, F79, M82, D84, M87, L95, W96, P97, and P98 of Ad2 E3/19K were replaced by alanine codons (Fig. 1). The Ad2 *Eco*RI D fragment inserted in the pBluescript II KS-vector (Stratagene, La Jolla, CA) served as a template for the first PCR carried out in two separate reactions, each using one mutagenesis-oligonucleotide (listed in Supplemental Table 1) containing the mutation (either sense or antisense) and one flanking oligonucleotide binding either 3′ or 5′ from the mutagenized site. The two partially overlapping products combined served as template for the second PCR using the flanking primers only to give rise to a ≈1200-bp fragment carrying the single amino acid mutation. After digestion with *Pac*I and *Sty*I (mutants E5–V64) or *Sty*I and *Bcl*I (mutants F77–P98) the corresponding fragments of 437 bp or 376 bp, respectively, were ligated into pBS-Ad2*Eco*RI D previously cleaved with the respective enzymes. The correct sequence of each mutant was verified by sequencing the portion of E3/19K amplified by PCR.

Cell lines and culture conditions

Two hundred ninety-three cells (ATCC CRL 1573) stably expressing Ad2 wild-type (Wt) E3/19K (293E3-45 or 293E3-22.7) were generated by transfection of 293 cells with the Ad2 *Eco*RV C and *Eco*RI D fragments, respectively (30, 60). In these plasmids E3 expression is driven by the natural E3 promoter that is stimulated by Ad E1A present endogenously in 293 cells. The 293E3-45 expresses all E3 proteins, whereas 293E3-22.7 only expresses E3A proteins, including E3/19K. As the *Eco*RI D fragment present in these cells lacks the second downstream poly A site, 293E3-22.7 cells only express ~50–60% of the amount of E3/19K as compared with 293E3-45 (16, 60, 61). Cell lines expressing E3/19K mutants E5, P9, T14, K27, I37, K42, W52, G55, Y60, V62, V64, M82, M87, W96, and P97 were established by transfection of 293 cells with mutagenized Ad2 *Eco*RI D fragments. Culture of 293 cells, transfection, and subsequent selection was performed as described (30, 62).

mAbs and antisera

The following mAbs were used: W6/32; anti–HLA-A, B, C (ATCC HB95); BB7.2, anti–HLA-A2 and Aw69 (63); 6D4, anti-MICA/B (BD Biosciences, San Jose, CA) or obtained from V. Groh (64), and BAMO3, anti-MICA/B (65). Tw1.3 (21) recognizes a discontinous, conformational epitope in Ad2 and Ad5 E3/19K. 3F4, 3A9, and 10A2 are specific for Ad2 E3/19K (57). Their epitopes were mapped to aa 3–13 (10A2), 15–21 (3A9), and 41–45 (3F4). For production of 3F4, 3A9, and 10A2, mice were immunized with a bacterially expressed His-tagged form of Ad2 E3/19K (57). To quantify E3/19K expression in the mutant cell lines by immunoprecipitation the polyclonal antiserum C-tail raised against the cytoplasmic tail peptide (aa 128–142) of Ad2 E3/19K (30) was used. The

reactivity of this antiserum seems unaffected by mutations within the ER-lumenal domain of E3/19K.

Transfection of cells

Transient transfections were performed using the calcium-phosphate method. A total of 6 μg plasmid DNA was resuspended in 90 μl TE (10 mM Tris/HCl pH 8.0/1mM EDTA) and 100 μl 2× HBS buffer (50 mM Hepes pH7.05, 140 mM NaCl, 1.5 mM Na_2HPO_4) was added. Thereafter, 10 μl 250 μM $CaCl_2$ was added under constant vortexing. After 5 min of incubation, the precipitate was added to a subconfluent monolayer of 293 cells (6-cm dish), and cells were analyzed 48 h thereafter. To generate 293 cell lines stably expressing mutant E3/19K proteins, plasmids carrying the mutations were cotransfected together with the pGCneo 635 plasmid conferring G418 resistance using electroporation. Prior to transfection, both plasmids were linearized using the restriction enzymes *Sal*I or *Sca*I for pBS-Ad2*Eco*RI D and *Pvu*I for pGCneo 635. The procedure for transfection and selection has been described previously (30). After ~14 d, G418-resistant clones were harvested and screened for E3/19K expression by flow cytometry (FACS) in the presence of saponin using a mixture of mAbs Tw1.3, 3A9, and 3F4, or by separate incubation with 3A9 and Tw1.3.

Cell labeling, immunoprecipitation, endoglycosidase H treatment, and SDS-PAGE

Labeling of cells with ^{35}S-methionine, immunoprecipitation with protein A-Sepharose, and SDS-PAGE have previously been described in detail (19, 24). Cells were lysed either in 1% NP40 or 1% digitonin. In the latter case, immunoprecipitates were washed in buffers containing 0.1% digitonin. Endoglycosidase H (endo H) treatment of HLA-A2 Ags was performed exactly as described (30). Radioactive proteins were quantified by phosphoimager (BAS 1000, FUJIX, Tokyo, Japan) analysis.

Flow cytometry

FACS was performed essentially as described (16, 30), except that 3–5 × 10^5 cells were used. Cells were stained with hybridoma supernatants or 1 μg purified mAb directed to E3/19K, HLA-I (W6/32) or MICA/B (6D4 or BAMO3). Thereafter, cells were either stained with FITC-conjugated goat anti-mouse IgG (1:50 dilution, Sigma-Aldrich, St. Louis, MO) or a 1:100 dilution of AlexaFluor 488-conjugated goat anti-mouse IgG (A11001, Life Technologies, Rockville, MD). To assess the expression of intracellular E3/19K all incubations except for the last resuspension step were conducted in the presence of 0.1% saponin. Fluorescence profiles were obtained by analyzing 5000 viable cells in a FACScan flow cytometer (BD Biosciences).

Bioinformatics

SNAP (58, 59) was used to predict the functional effects of alanine substitutions in the luminal domain (residue 1–100). For the cysteines, the effect of serine substitutions was investigated. SNAP is a neural network-based method that uses sequence-only inputs to return a binary prediction of functional effect (neutral/non-neutral) and raw scores for each substitution (ranging from −100 to +100; server implementation of SNAP returns reliability indices [RI] computed directly from raw scores). At default, neutral predictions are negative (≤0) and non-neutral predictions are positive (>0). The overall classification accuracy of SNAP has been reported as 79% (59) for a test set of >80,000 mutants with experimentally determined functional effects. SNAP performed slightly worse for the subset of >11,000 transmembrane protein mutants [~73% accuracy (66)]. SNAP scores are correlated with expected accuracy of prediction as calculated in testing on the original data. Higher scores of non-neutral predictions are also somewhat correlated with expected severity of change.

Results

Mutations of conserved amino acids in E3/19K differentially affect coprecipitation with HLA-I molecules in transiently transfected 293 cells

Despite the functional conservation of E3/19K proteins, their amino acid sequences are markedly variable among Ad species (5, 10). Only 20 aas within the luminal domain of 104–115 aas are strictly conserved in E3/19K molecules of different human Ad species (Fig. 1, thick arrows plus cysteines). Another 23 positions are highly conserved with only a single exchange found in one of the Ad species. It is postulated that these conserved amino acids are critical for structural integrity and functional activity of E3/19K. To test this hypothesis, we now have performed alanine scanning mutagenesis of the Ad2 E3/19K protein, replacing each strictly conserved amino acid plus five highly conserved amino acids by alanine (thin arrows). The four strictly conserved cysteines in the luminal domain

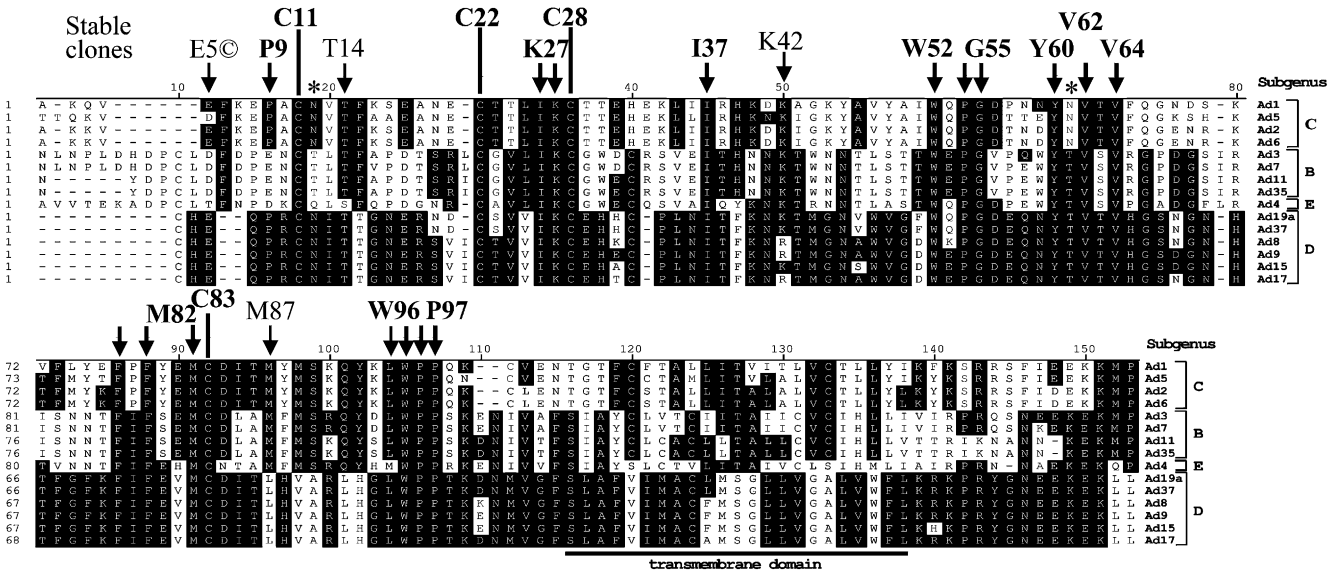

FIGURE 1. Amino acid sequence comparison of E3/19K proteins encoded by Ads from different subgroups. Alignment of E3/19K amino acid sequences from species B–D Ads. With the exception of species E (only one existing serotype) at least four sequences are shown. Reprinted with permission from Burgert et al (5). Sequences of the mature proteins with putative signal sequences omitted are shown. The consensus sequence is highlighted by black shading. Dashes indicate absent residues. The strictly and highly conserved amino acids within the luminal domain mutated here are indicated by thick and thin arrows, respectively. Introducing an additional gap after P9 and P5 in the species C and D sequence, respectively, makes P9 also strictly conserved. Mutants from which stable clones have been generated are denoted with the single letter code and the position in bold, for strictly conserved amino acids, and in plain for highly conserved amino acids. The conserved cysteines in positions 11, 22, 28, and 83 mutated previously are also indicated. E5© denotes the nonconserved glutamic acid that was analyzed as control. The transmembrane region and the glycosylation sites in Ad2 E3/19K are highlighted by a line below and asterisks above the sequences, respectively.

have been analyzed previously (15, 30). The Ad2 protein was chosen because four mAbs and an antiserum against the cytoplasmic tail were available, allowing us 1) to detect all mutants and 2) to relate potential functional alterations to changes in conformation. The neutral amino acid alanine was selected to keep the impact on structural integrity to a minimum. As a first screen for functional activity, mutant E3/19K genes were transiently transfected into 293 cells. The ability of the mutant proteins to bind HLA-I was examined by metabolic labeling and coprecipitation using mAb W6/32. As the extent of HLA complex formation is dependent on the amount of E3/19K expressed, which is mainly determined by the transfection efficiency, the expression level of E3/19K was controlled with the C-tail serum. To obtain preliminary information about potential conformational changes, E3/19K was also precipitated with the conformation-sensitive mAb Tw1.3 that recognizes a discontinuous epitope (21, 57). Examples of directly precipitated E3/19K using C-tail serum and Tw1.3 as well as coprecipitated E3/19K are shown in Fig. 2*A*. As expected, the expression level of E3/19K varied considerably, being low for example, for Wt, K42, W52, and Y60 and higher for most other mutants. When this is taken into consideration striking differences of the mutations on the level of coprecipitation were revealed (Fig. 2, W6/32 [W]; compare, for example, I37, V64, and M87 with F77, F79, and L95). To verify these data, the experiment was repeated and the fluorographs were quantitatively analyzed by phosphoimager analysis. The amount of coprecipitated E3/19K was related to the total amount of E3/19K as determined by immunoprecipitation with the C-tail serum and the ratio obtained for Wt E3/19K was set to 100% (Fig. 2*B*). Likewise, the relative binding affinity of Tw1.3 to the different mutants is expressed as the ratio of radioactivity detected in the E3/19K-specific bands of the Tw1.3 precipitate versus that by C-tail and the ratio obtained for WT E3/19K was set to 100% (Fig. 2*C*). The quantitative analysis derived from 1–3 experiments illustrates the differential effect of the mutations on HLA-I binding. A number of mutants had completely lost the ability to bind to HLA-I (I37, W52, V64, and M87), others showed modest reductions (e.g., P9, I26, K42, Y60, and P97) and again others hardly any negative effect (i.e., F79, M82, L95, and P98). These minor effects were unexpected considering that we had mutated conserved amino acids. Also, the amino acids, the mutation of which lead to the most devastating effect on HLA-I binding of E3/19K (I37, W52, V64, M87, and W96) are not concentrated in a particular part of the sequence, but are widely distributed throughout the luminal domain. Furthermore, there is no correlation between Tw1.3 reactivity and HLA-I–binding activity. Precipitation with mAb Tw1.3 revealed differential effects of the mutations on the integrity of the conformational epitope (Fig. 2*C*). For example, although mutants I37 and V64 no longer bound Tw1.3, all mutants from F77 to P98 representing the so-called "conserved domain" were recognized with similar binding efficiency as Wt (56, 57).

Generation and structural characterizaton of stable transfectants from a selected set of E3/19K mutants

Coprecipitation of E3/19K mutants with HLA-I is only a first criterion for functional activity, particularly in combination with transient transfections because these are prone to some variation because of differences in transfection efficiency. To verify the above data and to enable a more detailed analysis of E3/19K function, such as inhibition of HLA-I transport and suppression of cell surface expression, we selected mutants with $<$50% binding activity to HLA-I in the transient assay for establishment of stable transfectants. Additional mutations were included, for example, the mutation of the nonconserved aa E5 that served as a negative control. As some mutations had a profound effect on Tw1.3 binding [Fig. 2*C*; and (57)], we screened the transfectants by intracellular flow cytometry using a mixture of mAbs Tw1.3, 3A9, and 3F4 in the presence of the detergent saponin. Each of these mAbs binds to different epitopes within E3/19K, therefore increasing the chances for successful detection of E3/19K mutants. From the 6–8 clones initially selected for further analysis, 2–5 with expression levels similar to the Wt expressing clones were chosen for subsequent experiments. Immunoprecipitation with the mutation-independent antiserum C-tail indeed confirmed a similar expression level to the Wt expressing clones 293E3-22.7 and 293E3-45 (Fig. 3). Furthermore, immunoprecipitations with mAbs Tw1.3, 3A9, and 3F4, were used to characterize structural alterations associated with the individual mutants. Generally, Wt E3/19K is most efficiently precipitated by mAb Tw1.3, followed by 3A9 and the C-tail antiserum although it lacks significant reactivity to 3F4. A similar pattern is seen for mutants E5 (control mutation of a nonconserved amino acid), T14, M87, and W96 (Fig. 3), whereas mutants P9, I37, W52, G55, Y60, V62, and V64 exhibited a 7–22-fold enhanced binding to mAb 3F4 [see also (57)]. This indicates that the 3F4 epitope comprising aa 41–45 and predicted to be on an internal loop between two β-strands becomes exposed by these mutations. In all these mutants, except W52 and G55, enhanced 3F4 binding was accompanied by a significant reduction or even loss (i.e., I37, V64) of Tw1.3 binding, suggesting considerable structural changes. By contrast, binding of mAb 3A9 to its epitope on the loop comprising aa 15–21 was not significantly altered, except for T14 and K27, which harbor changes in the vicinity of the epitope. Of note is the difference in the apparent molecular weight of mutant T14 compared with Wt and the other mutants. This is explained by the elimination of the *N*-linked glycan at position 12 by the T14A mutation as this residue is part of an *N*-glycosylation site NVT_{14} that is destroyed by the mutation.

First criterion for E3/19K function: HLA-I–binding activity of stably expressed E3/19K mutants

Two clones from each mutant with a similar expression level of E3/19K as in Wt expressing clones were tested for their ability to bind to HLA-I. Extracts of ^{35}*S*-methionine–labeled cells were precipitated with the HLA-I specific mAb W6/32 (Fig. 4*A*, 4*B*). Coprecipitation depends on the binding activity of the E3/19K mutant, its expression level, the expression level of HLA-I in that clone, and the amount of HLA-I precipitated. As before, coprecipitated E3/19K was related to the total amount of E3/19K precipitated by the C-tail serum. In general, the data obtained with stable clones corroborated those obtained after transient transfection (see Fig. 2*B*). Mutants that did not exhibit significant binding to HLA-I in the latter also turned out to show no (I37, W52, V64, and M87) or very little (W96) binding activity in stable transfectants (Fig. 4*A*, compare *lanes 1–3* with *lanes 12–13* and *lanes18–19*; 4*B*, compare *lanes 1–3* with *lanes 8–13*). By contrast, alanine mutants generated from the nonconserved aa E5 (control mutant) or from T14 were coprecipitated to a similar extent as Wt E3/19K. In agreement with the transient transfection data, the remaining mutants showed reduced HLA-I complex formation. The average percentage of coprecipitated E3/19K from 2–3 experiments relative to WT is shown as normalized data in Fig. 4*C*. A comparison of the efficiency of coprecipitation in transient and stable transfectants of the same mutant revealed little variation (0–21%). The largest difference was observed for K42 (21.1%) and V62 (17.8%). These results indicate that the HLA-I binding data determined in transient and stable transfections are comparable, hence, the transient assay appears to constitute a reliable screen for assessing HLA-I–binding activity of E3/19K mutants. Taken together, the mutants may be classified in three groups: 1) mutants such as I37, W52, V64, M87, and W96 that lost HLA-I binding by $>$90% as compared with Wt 2) mutants exhibiting intermediate

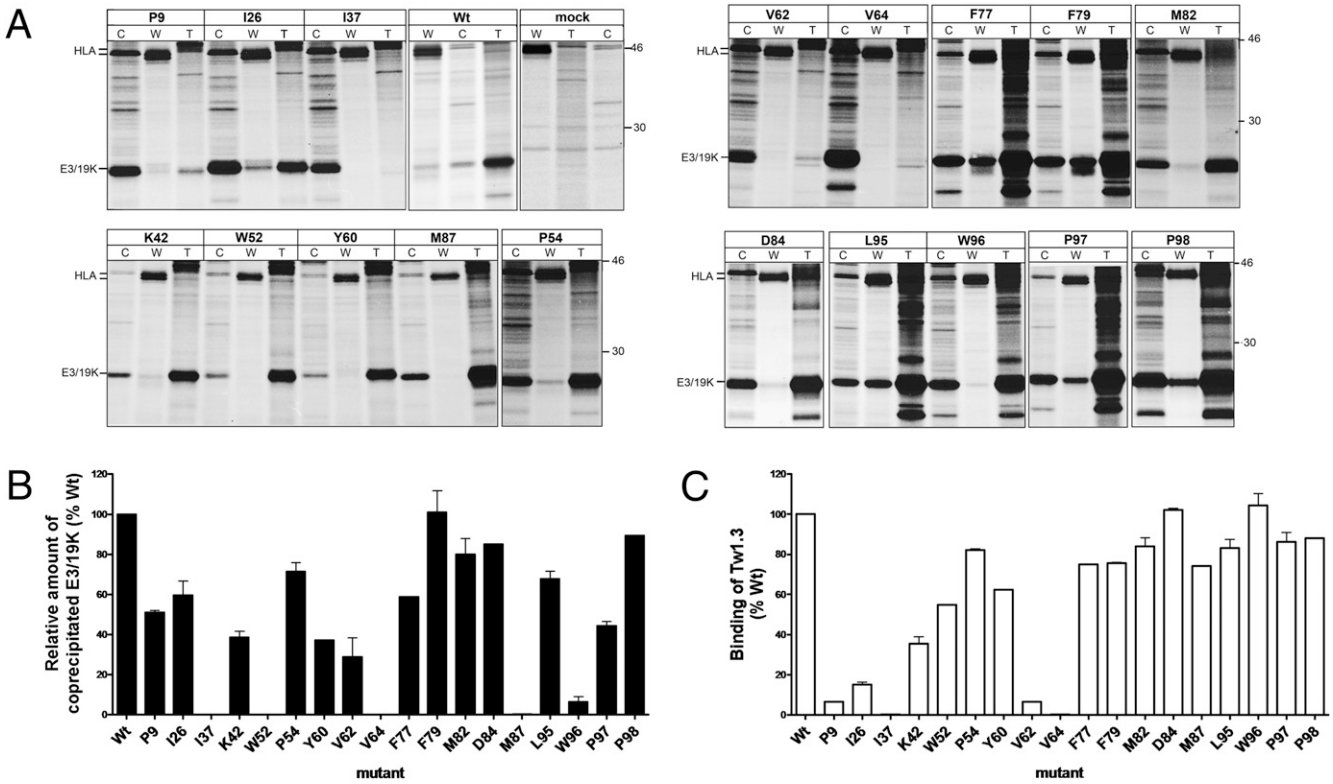

FIGURE 2. HLA-I binding of E3/19K mutants and reactivity with mAb Tw1.3 after transient transfection, metabolic labeling and immunoprecipitation. Two hundred ninety-three cells were transiently transfected with Wt and mutant pBS-Ad2*Eco*RI D constructs using calcium phosphate precipitation. 45–48 h posttransfection cells were labeled with 100 μCi/ml ^{35}*S*-methionine for 3 h. Digitonin lysates of cells were divided in three equal parts and incubated with Abs C-tail (C), Tw1.3 (T), and W6/32 (W). Examples shown in *A* are collated from three independent experiments. As control, Wt E3/19K was analyzed in each experiment, but only shown once. In addition, immunoprecipitations of mock transfected cells are shown. The mutants analyzed are given on top. The position of the HLA-I species (HLA) and E3/19K protein (E3/19K) is marked on the left, that of molecular weight markers (GE Healthcare, Munich, Germany) on the right. The relative radioactivity in the M82 and M87 mutants is lower due to the loss of one of the five methionines by the mutation. However, as the E3/19K species in W6/32 and Tw1.3 precipitates were related to C-tail, this did not affect the analysis. Mutants E5, T14, K27, and G55 were only analyzed as stable clones (see below). *B*, Quantitative analysis of HLA-I binding by Wt E3/19K and alanine replacement mutants on transient transfection. The association with HLA-I of Wt and mutants was quantitatively assessed by measuring the amount of radioactive E3/19K coprecipitated by W6/32 using a phosphoimager. Binding to HLA-I of the different mutants relative to Wt is expressed as the ratio of radioactivity detected in the coprecipitated E3/19K band versus that by C-tail, with the ratio obtained for Wt E3/19K set to 100%. *C*, Binding of mutants to the conformation-dependent mAb Tw1.3 relative to Wt E3/19K. The ratio of E3/19K-specific radioactivity was calculated from the amount of radioactivity in the E3/19K species precipitated by Tw1.3 and C-tail. Bars represent the mean of at least two independent experiments.

binding activities (11–79%; P9, K27, K42, G55, Y60, V62); and 3) mutants such as T14, F79, M82, D84, and P98 with essentially unaltered binding activities (differences to Wt <20%).

Second criterion for E3/19K function: influence of mutations on HLA-I transport

Coprecipitation depends on a number of factors, and as E3/19K may inhibit transport of HLA-I alleles with low affinity to E3/19K indirectly by binding to TAP, thereby impairing the recruitment of HLA-tapasin complexes to TAP and peptide loading (36, 67), coprecipitation alone may not be a reliable measure for E3/19K activity. Thus, a lack of coprecipitation does not necessarily indicate a lack of transport inhibition [(68); H.-G. Burgert, unpublished observation]. To directly assess HLA-I transport through the medium/*trans*-Golgi apparatus in cells expressing mutant E3/19K, the acquisition of complex carbohydrates by HLA-I was determined in pulse–chase experiments. Acquisition of complex carbohydrates results in endo H resistance of HLA-I and is indicative of transport through the medium/*trans*-Golgi apparatus. To facilitate the analysis and detect the small molecular weight changes associated with the conversion of high mannose sugars to complex type carbohydrates, the analysis was restricted to one allele, HLA-A2, which exhibits high affinity to Ad2 E3/19K (41, 42, 44, 45). After pulse-labeling for 20 min cells were chased in an excess of unlabeled methionine for 2.5 h. In untransfected 293 cells, HLA-A2 undergoes a small shift in apparent molecular weight (Fig. 5, *lanes 1* and *2*). This latter species is endo H resistant, whereas the pulsed sample is cleaved (Fig. 5, *lanes 3* and *4*). By contrast, HLA-A2 molecules in 293E3-45 cells expressing Wt E3/19K remain endo H sensitive throughout the chase period, indicating complete transport inhibition (Fig. 5, *lanes 5* and *6*). A similar transport inhibition is noted for mutants E5, T14, and K27, whereas a significant fraction of endo H–resistant HLA-A2 is observed in mutants K42, G55, Y60, and V62. A greater percentage of mature HLA-A2 is found in W52 (~35%) and P9 (~65%), whereas in four clones (M87, W96, I37, V64), essentially all HLA-A2 became endo H resistant within the 2.5-h timeframe (Supplemental Fig. 1*B*). These latter E3/19K mutants have apparently lost the ability to retain HLA-A2. With the exception of mutant W52, that showed some degree of transport inhibition in the absence of direct evidence for strong HLA-I binding the results of the pulse–chase experiments correlate well with the coprecipitation data (Fig. 4). For some mutants (P9, I37, K42, V62, V64, M87, W96), we also assessed the acquisition of endo H resistance of the HLA-I alleles remaining in the lysates after HLA-A2 immunoprecipitation (mostly

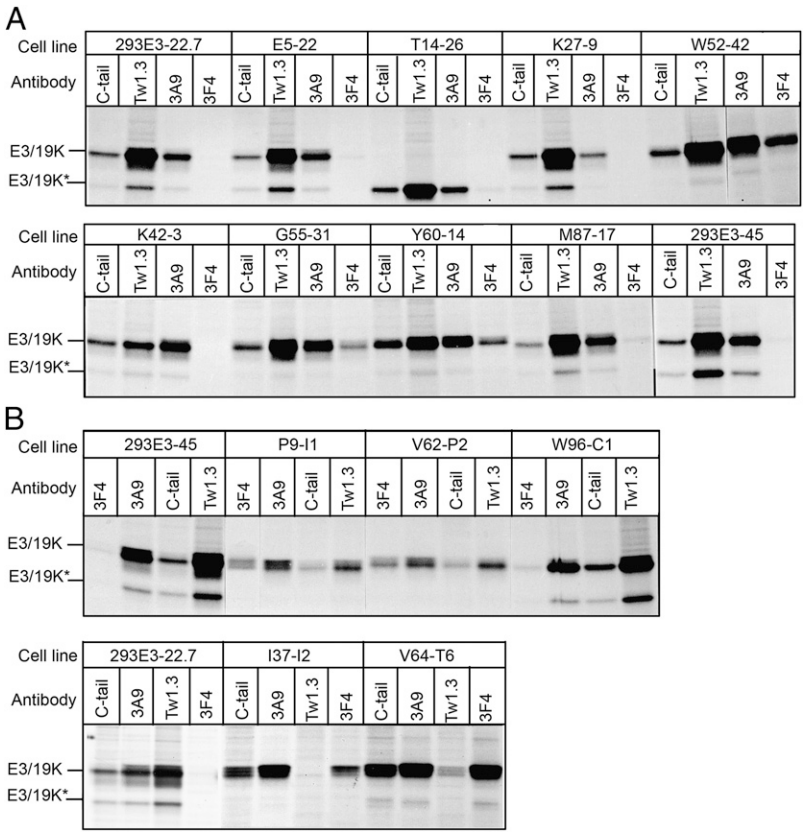

FIGURE 3. Relative binding activity of mAbs to alanine replacement mutants of E3/19K. The binding efficiency of the mAbs Tw1.3, 3A9, 3F4, and the C-tail antiserum to the various E3/19K mutants was determined by immunoprecipitation. Stable 293 transfectants expressing the mutants indicated on top were labeled with 100 μCi/ml ^{35}S-methionine for 1 h and lysed in 1% NP40 lysis buffer. Equal amounts of lysate were used for immunoprecipitation with the mAbs Tw1.3, 3A9, 3F4, and C-tail serum denoted on top. The amount of radioactive E3/19K precipitated by the Abs (see also Fig. 2) was quantitatively determined by phosphoimager analysis. E3/19K∗ marks monoglycosylated E3/19K that is present in all immunoprecipitates at a low level, but is the exclusive species in the T14 expressing clones. Two independent experiments including the control cell lines 293E3-22.7 and 293E3-45 were carried out and are shown in *A* and *B* .

HLA-B/C; Supplemental Fig. 1*A*, 1*B*, and data not shown). In general, the resistant HLA fraction is nearly identical to that seen for HLA-A2 (differences of ~10%), except for mutant V62 where only 15% of HLA-A2 molecules were transported as compared with 50% of HLA-A2 depleted HLA-I. FACS analysis confirmed a differential expression of HLA-A2 and HLA-I on the cell surface of V62 mutant cell lines, whereas their expression did not significantly differ in all other mutants tested (Supplemental Fig. 1*C* and data not shown). It remains to be seen whether the V62 residue is more critical for the retention of HLA-B/C alleles as compared with HLA-A2.

Third criterion for E3/19K function: influence of mutations on steady-state HLA-I cell surface expression

The pulse–chase experiments represent a kinetic snapshot of the effect of the mutation on inhibition of HLA-A2 transport. Because of the differential association of HLA-I alleles with E3/19K, the cell surface expression of HLA-I at steady state cannot be inferred from these experiments. Therefore, HLA-I cell surface expression of cell clones expressing E3/19K mutants was quantitatively compared with that in Wt expressing clones and untransfected cells using flow cytometry. As the intrinsic expression of HLA in the individual clones may vary, we have tested a minimum of three clones from each mutant in at least two independent experiments. Typical histograms of selected mutants are shown in Fig. 6*A*, and the calculated mean fluorescence intensity relative to E3/19K-negative 293 cells is shown in Fig. 6*B*. Whereas HLA-I expression in Wt E3/19K expressing clones is reduced by >80% compared with 293 cells, little or no downregulation was observed in mutants P9, I37, W52, V62, V64, M87, and W96. These data are in line with the coprecipitation data and correlate with the pulse–chase data, therefore, these amino acids seem crucial for HLA-I modulation. In mutants E5, T14, K27, and M82, the suppression of HLA-I is only minimally compromised, whereas two other mutant cell lines (K42 and G55) exhibit an intermediate HLA-I cell surface level, correlating well with the reduced coprecipitation of these mutants with HLA-I (reduction by 40% and 31%, respectively). Taken together, a strong correlation exists between the three criteria for E3/19K function, namely, HLA-I binding, transport inhibition, and suppression of HLA-I cell surface expression. Interestingly, however, for mutants with a moderately reduced HLA-I–binding capacity (reduction of 60–40% in coprecipitation), small differences in binding seem to have a profound impact on steady-state HLA-I surface expression.

Fourth criterion for E3/19K function: effect of mutations on MICA/B cell surface expression

The discovery of a new functional activity of E3/19K, downregulation of the stress molecules MICA/B (15), prompted us to test whether the mutations affected the capacity of E3/19K to downregulate MICA/B in a similar way as HLA-I (Fig. 6*C*). By and large, the mutations have a lesser impact on MICA/B downregulation than on HLA-I. However, there are significant differences among the mutants that suggest they might be classified in different groups depending on their effect on both target molecules. The classification scheme used in this study was based on the ratio between the HLA and MICA/B cell surface expression for each mutant, which is 0.67 and 0.85, respectively, for the two E3/19K Wt expressing clones. As expected, the mutation of the nonconserved aa E5 hardly affected either E3/19K function (HLA/MICA/B ratio, 0.98). We consider mutants with an HLA/MICA/B ratio <1.8 as those where the altered amino acid has a similar functional relevance for both HLA-I and MICA/B downregulation. This group comprises P9 (1.39), I37 (1.72), G55 (1.57), Y60 (1.18), V62 (1.08), and V64 (1.75). A second set of mutations preferentially compromises the ability of E3/19K to downregulate HLA-I with relatively little impact on MICA/B downregulation (HLA/MICA/B ratios >1.8). These include mutants K27 (2.38), K42 (2.34), W52 (2.37), M87 (4.17), W96

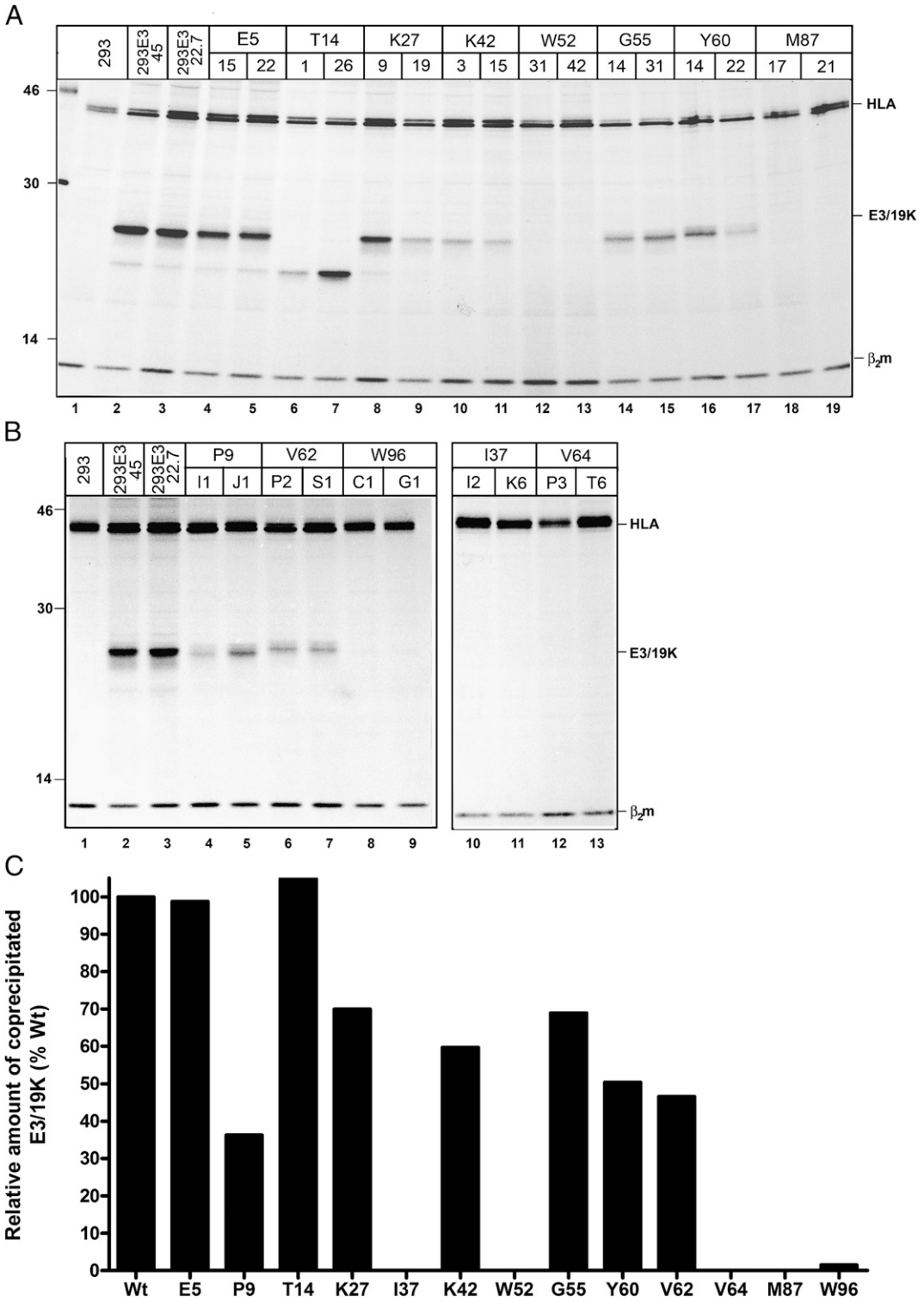

FIGURE 4. Capacity of E3/19K mutants to form complexes with HLA-I in cell clones stably expressing the mutants. Two cell clones of each mutant along with the control cell lines 293, 293E3-22.7, and 293E3-45 were labeled with 100 μCi/ml of ^{35}S-methionine for 1 h. NP40 lysates were immunoprecipitated with mAb W6/32 directed against HLA-I. Corresponding autoradiographs are shown in *A* and *B*. Positions of HLA-I heavy chains (HLA), E3/19K, and β_2-m are marked on the right, those of molecular weight markers (kDa) on the left. *C*, The amount of coprecipitated E3/19K was determined by phosphoimager analysis and related to that found in cell lines expressing Wt E3/19K as described for Fig. 2*B*.

(1.93), and P97 (2.0). A third group with a reverse phenotype consists of mutants M82 (0.32) and T14 (0.37) that lost the *N*-linked glycan at position 12. Both mutations severely compromise the capacity of E3/19K to downregulate MICA/B while leaving downregulation of HLA-I largely intact. If we use an alternative classification scheme based on the percentage difference between the relative HLA-I and MICA/B expression, taking <35% difference as a cutoff for a similar functional effect on both target molecules, the grouping remains the same, except that K27 (23%) would be considered as mutant with a similar impact on both target molecules, whereas I37 (47%) and V64 (49.6%) would have a preferential impact on HLA. Whatever system is used, the data

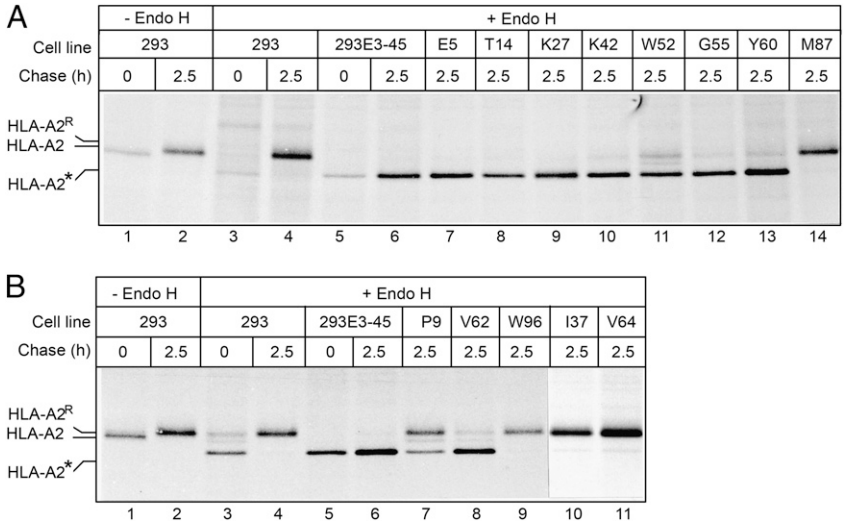

FIGURE 5. Transport of HLA-A2 in cells expressing mutant and Wt E3/19K molecules. The 293, 293E3-45, and mutant cell lines were pulse-labeled for 20 min with 200 μCi/ml ^{35}S-methionine, chased for 2.5 h in an excess of cold methionine and lysed (*A*, *lanes 2, 4, 6–14; B*, *lanes 2, 4, 6–11*). In addition, samples of 293 cells and 293E3-45 cells were lysed directly (0) after the pulse (*A* and *B*, *lanes 1, 3, 5*). HLA-A2 molecules were immunoprecipitated using mAb BB7.2. Immunoprecipitated material was treated with endo H (+endo H; *A*, *lanes 3–14*, *B*, *lanes 3–11*), except the material loaded in *lanes 1* and *2,* which was mock-treated. The positions of the HLA-A2 heavy chain carrying high mannose glycans (HLA-A2), the endo H resistant HLA-A2 species (HLA-A2^R) and the endo H cleaved HLA-A2 species (HLA-A2∗) are marked on the left.

suggest that some amino acids may have a differential role for downregulation of the two E3/19K target proteins.

Functional relevance of residues as determined by prediction of nonneutral versus neutral effects of mutations

Our selection of amino acid positions for mutation was based on their conservation among Ads. To validate this selection and to examine the putative functional relevance of other amino acids in E3/19K, we used a neural network-based method, coined "SNAP," for predicting functional effects of single amino acid substitutions in sequence (59). The inputs to the network include a number of protein features (predicted from sequence) local to the given position (i.e., solvent accessibility, secondary structure, and native chain flexibility), as well as biochemical differences between the original and the inserted residues. The network was trained on a large set of known mutants with experimentally annotated functional effects. SNAP makes predictions as to whether a mutation constitutes a functional nonneutral or neutral exchange. In the context of the SNAP analysis, we considered an increase in cell surface expression of HLA-I or MICA/B of >33% over cells expressing Wt E3/19K as significant functional change and as threshold for signifying a nonneutral change. Similarly, a reduction of coprecipitation by >33% was considered a nonneutral change. When we compared our results with the effects predicted by SNAP for the alanine substitutions we found a large degree of agreement (Fig. 7*A*). Overall, of 26 positions (including the four conserved cysteines) investigated, 19 predictions were correct, yielding an overall accuracy of 73%, which is in complete agreement with the 73% accuracy of SNAP for predictions of transmembrane proteins (66). For example, SNAP predicts a neutral change (score: −12) for the mutation of the nonconserved control residue E5, and accordingly this mutation was experimentally shown to be neutral with regard to function. In contrast, most mutants investigated in this study, for example, I26 (score: 32), W52 (score: 55), Y60 (score: 39), V62 (score: 48), and V64 (score: 47) have high-positive scores, suggesting nonneutral changes (Fig. 7*A*). High-reliability nonneutrality scores, suggesting profound (nonneutral) functional alterations, are predicted for all conserved cysteines, which has been verified in our previous study (30). It appears that at least in part even quantitative functional changes may be predictable, for example, the experimentally determined changes are smaller for G55 (score: 27) and P54 (score: 8) than for either of the above mentioned deleterious mutations. For a few positions (P9, K27, P54, F79, D84, L95, and P98), SNAP did not correctly predict the outcome, for example, the predicted neutral P9A mutation (score: −10) almost completely abrogated E3/19K function. In contrast, the K27A substitution predicted to produce a nonneutral phenotype resulted only in minor changes of activity (Fig. 6). Interestingly, the other mutants with incorrect predictions have only been analyzed in the transient HLA binding assay.

As mutation of some residues results in functionally disparate effects on the two E3/19K target proteins, the comparison between prediction and functional alteration becomes more complex. For instance, the T14A (score: 47) substitution had no significant effect on HLA-I downregulation, but essentially abrogated intracellular sequestration of MICA/B. On the other hand, M87A (score: 40) was very benign with respect to MICA/B downregulation, but was functionally disruptive as witnessed by reconstitution of HLA-I cell surface expression. Fig. 7*B* shows the SNAP predictions for all residues in the luminal domain of E3/19K. It is remarkable that more than half of all amino acid changes are predicted to be nonneutral with relatively high reliability (54% with a score >10). However, when taking a cue from experimental results to reset the threshold of functional effect (lowest SNAP score for experimentally determined nonneutral mutant is 24 for P97), the number of residues annotated as functionally important was reduced to 33 of 100 (33%).

Discussion

Based on the hypothesis that conserved amino acids are functionally important, we have systematically substituted alanine for all 16 strictly conserved and 5 highly conserved amino acids in the ER luminal domain of Ad2 E3/19K. A schematic drawing of this domain incorporating the secondary structure prediction (57), the approximate position of the mAb binding sites and that of the conserved amino acids analyzed in this study are shown in Fig. 8. Previous studies using deletion or mutagenesis of the cysteines revealed that this domain is crucial for binding to HLA-I (30, 53). Using a sensitive transfection system that is not influenced by cytokine effects on HLA-I/MICA/B expression induced by viral infection, and the kinetic issues of an infection system (time to express E3 proteins, time to detect significant downregulation of HLA-I/MICA/B), we show that the mutations induce a variety of phenotypes ranging from total loss of HLA-I downregulation (e.g., in I37, V62, or V64) to only minimal effects in the M82, T14, or K27 mutants. After an initial screen combining transient transfection with immunoprecipitation, we selected mutants that exhibited a >50% loss of HLA-I–binding activity in this assay for comprehensive functional characterization in stable transfectants. Functional activity of E3/19K was assessed using three criteria:

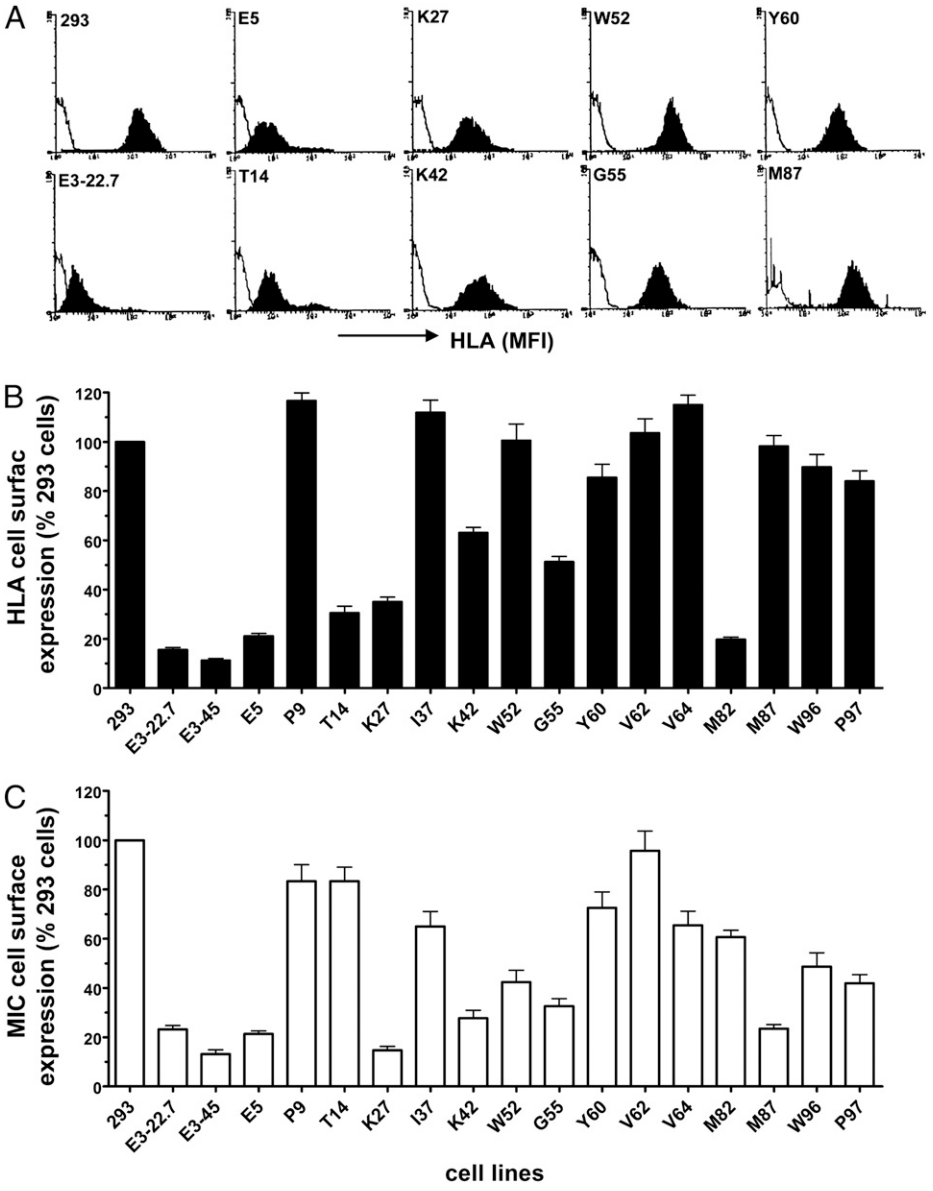

FIGURE 6. Cell surface expression of HLA-I and MICA/B in cells expressing mutant and Wt E3/19K molecules, or in E3/19K negative cells. *A*, HLA-I histograms of 293 cells, 293E3-22.7 cells and various cell clones expressing the E3/19K mutant given in the *upper left corner* are shown. Cells were stained for flow cytometry using mAb W6/32, followed by FITC-labeled goat anti-mouse IgG (solid histograms) or were incubated with FITC-labeled goat anti-mouse IgG alone (black line). *B*, Relative expression level of HLA-I and MICA/B (*C*) as measured by FACS analysis of 293 cells and cell clones expressing Wt or mutant E3/19K molecules using mAbs W6/32 and 6D4 or BAMO3, respectively. Cells were stained with the above mAbs, followed by incubation with Alexa 488-coupled goat anti-mouse IgG. At least four clones from each mutant with similar E3/19K expression as Wt expressing 293 cells were analyzed in at least 3–5 independent experiments. The background staining obtained with the secondary Ab alone was deducted and the mean fluorescence intensity related to that of 293 cells, which was arbitrarily set to 100%. Bars represent means and SEM.

(1) binding to HLA-I using coimmunoprecipitation, (2) inhibition of HLA-I transport as analyzed by pulse–chase experiments, and (3) inhibition of HLA-I cell surface expression using quantitative flow cytometry. In addition, the effect of the mutations on the cell surface expression of the newly discovered E3/19K target proteins MICA/B was assessed. We are confident that the data obtained in this study with the transfection system are also relevant for the Ad2 infection because comparable functional data were obtained for the W96A E3/19K mutant that was analyzed both in transfected cells and in the corresponding virus mutant (15).

In general, consistent data were obtained with these three assays. Mutants that exhibited a similar HLA-I–binding activity as Wt, such as T14 and K27, or the control mutant E5, representing an alanine substitution of a nonconserved residue, also retained the capacity to prevent the transport of HLA-A2 and to suppress steady-state expression of HLA on the cell surface. On the other hand, mutants that had lost HLA-I–binding activity such as I37, W52, V64, M87, or W96, were unable to suppress cell surface expression of HLA-I. Thus, we found little evidence that an E3/19K mutant that had lost HLA-I binding would indirectly interfere with HLA-I transport, for example, by binding to TAP (36). Only W52 fulfills to some extent the criteria of a TAP binding mutant (lack of coprecipitation, combined with HLA transport inhibition). However, the slower transport of HLA-A2 did not result in a reduced cell surface expression of HLA-A,B,C in different W52 cell clones at steady state. More direct experiments will need to be carried out to clarify whether this mutant may bind to TAP.

A good correlation between HLA-I binding and reduced HLA-I cell surface expression also existed for most mutants with a moderate effect on binding (e.g., K42, G55) whereby a coprecipitation efficiency of ~50% of Wt may represent a critical threshold, as small differences in the avidity of interaction (coprecipitation) may lead to considerable changes in HLA-I cell surface expression at steady state (Figs. 4*C*, 6, and data not shown). Minor differences in the three assays are to be expected because different numbers of cell clones were analyzed in each assay system. Considering, that HLA-A2 binds with high affinity to E3/19K (41, 44) and other alleles in 293 cells are likely to interact less avidly, the pulse–chase analysis of HLA-A2 is overestimating the effect of E3/19K on HLA-I transport.

Perhaps the most surprising result was that more than one-third of the mutants exhibited only relatively minor functional deficiencies

A

Position:	5	**9**[1]	11	14	22	26	**27**	28	37	42	52	**54**	55
Residue:	E	P	C	T	C	I	K	C	I	K	W	P	G
SNAP score:	-12	-10	48	47	49	32	51	48	36	47	55	8	27
Function disruption	-	+++	++	++[M]	++	+*	-	++	++	+	+++	-*	+

Position:	60	62	64	77	**79**	82	83	**84**	87	**95**	96	97	**98**
Residue:	Y	V	V	F	F	M	C	D	M	L	W	P	P
SNAP score:	39	48	47	51	53	39	56	49	40	32	36	24	30
Function disruption	+++	+++	+++	+*	-*	+[M]	++	-*	+++	-*	+++	++	-*

B

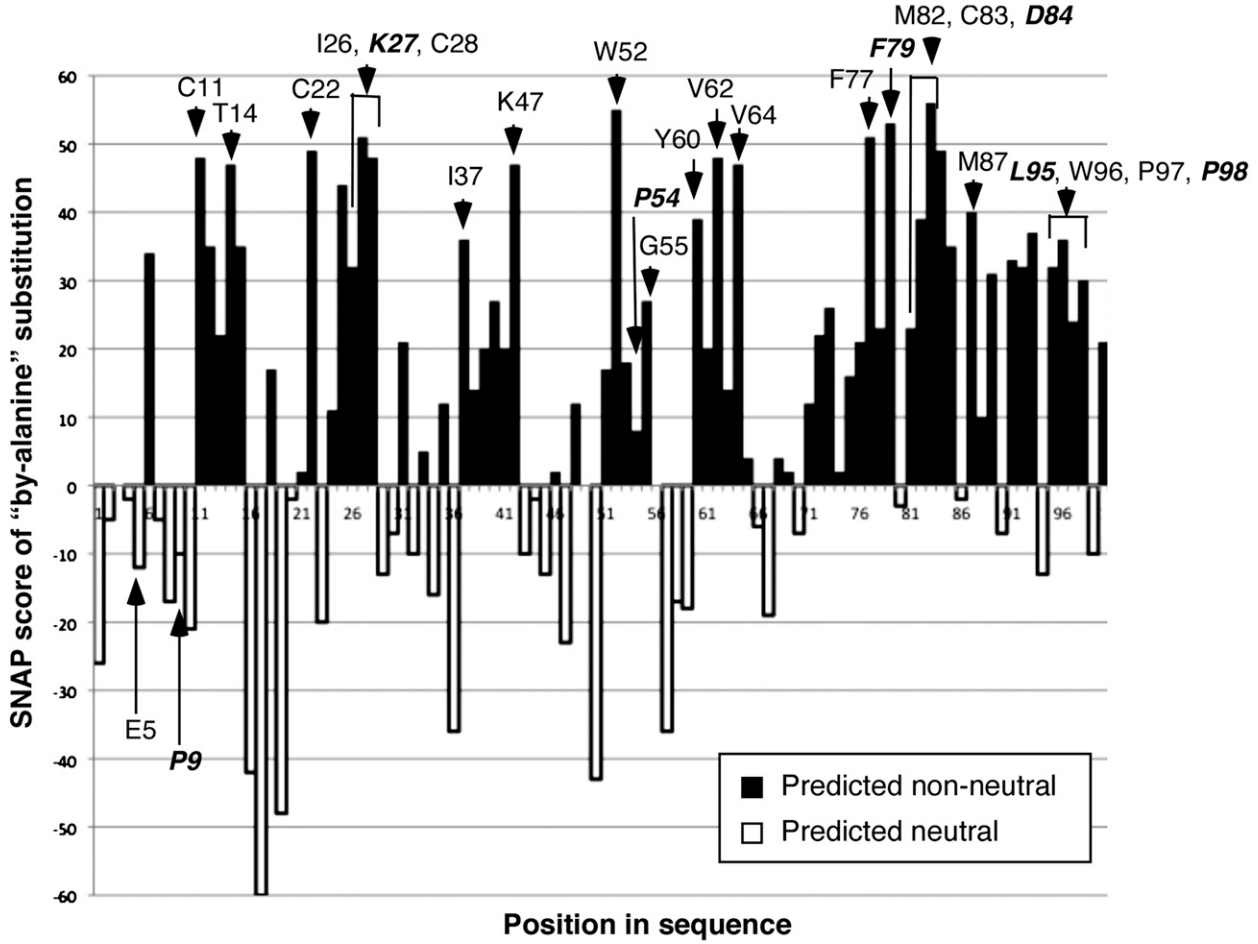

FIGURE 7. Comparison of SNAP score prediction with functional change. *A*, The position and the residue mutated is given together with the SNAP raw score and a semiquantitative indicator of functional disruption with (−) being none; (+), 33–50%; (++), 51–75%; (+++) >76%. A >33% change of MICA/B or HLA surface expression or reduction in coimmunoprecipitation is considered significant and as a threshold for a nonneutral change. Residues for which predictions did not correlate with functional data are indicated in bold. [M]: indicates that only MICA/B is functionally affected. ∗Based on coimmunoprecipitation in the transient assay. *B*, SNAP prediction for the luminal domain of Ad2 E3/19K, aa 1–100. Nonneutral changes are depicted as black bars above the zero line, neutral changes as white bars below the line. The *y*-axis represents the SNAP raw scores. Amino acid residues are given in italics and bold when SNAP did not predict the phenotype correctly.

as measured by HLA-I coprecipitation (I26, P54, F77, F79, D84, L95, and P98; Fig. 8, residues without shading) or FACS analysis (T14, M82; Fig. 8, dark gray). This suggested that these conserved amino acids are of lesser importance for the interaction with HLA-I. Although their critical importance for the interaction of E3/19K with HLA-I alleles not present in 293 cells cannot be excluded their conservation may imply an essential role for the interaction with other potential E3/19K target proteins. Interestingly, E3/19K was shown to increase complex formation of certain MHC-I alleles with the amyloid precursor-like protein 2, which has been implicated in peptide transfer (37, 69) and in modulation of the stability and endocytosis of some murine and human MHC-I alleles (70, 71). Also, some of these conserved amino acids might be important for the interaction with TAP or MICA/B.

In this study, we have examined the relevance of these conserved amino acids for MICA/B downregulation. To date, attempts to demonstrate a direct interaction between MICA/B and E3/19K have failed; therefore, we could not reliably test the above mutants by coimmunoprecipitation with MICA/B. However, all stable cell lines were tested for cell surface expression of MICA/B. Moreover, stable cell clones from mutant M82 that exhibited only minor deficiencies in the transient HLA binding assay showed essentially unaltered downregulation of HLA-I, whereas MICA/B downregulation was severely compromised. A similar phenotype was

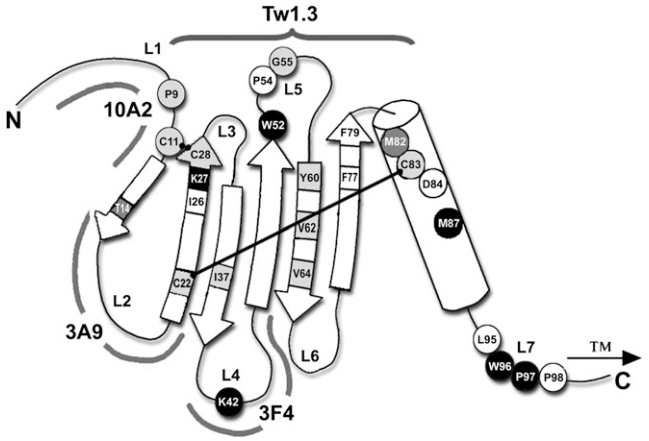

FIGURE 8. Schematic model of the ER luminal domain of the Ad2 E3/19K protein based on secondary structure prediction (57) showing the approximate positions of conserved amino acids and the binding sites of mAbs 10A2 (aa 3–13), 3A9 (aa 15–21), 3F4 (aa 41–46), and Tw1.3 (conformational). Light gray shading indicates amino acids the mutation of which had a similar effect on HLA-I and MICA/B surface expression. Black shading highlights amino acids that are primarily critical for HLA-I modulation, whereas amino acids marked with dark gray shading (T14, M82) affect predominantly MICA/B rather than HLA-I. Residues without shading indicate those with no drastic effect on HLA binding. The drawing is spread out to enable to show all relevant elements. We do not know the orientation of individual β strands (arrows) and the relative position of those to the α helix (column). [^{11}C] and C28, as well as C22 and C83, are connected via disulfide bonds (30), so in reality these form intimate contacts. L1-L7 indicate loop structures that may be recognized by the mAbs. The 10A2 and 3F4 epitopes are largely buried in the Wt molecule. The frequently similar but distinct changes in binding by these two mAbs suggests that their epitopes may be spatially close together. C, C terminus; N, N terminus; TM, transmembrane domain.

seen for T14 (Fig. 6*C* and Fig. 8, dark grey shading). The T14A mutation leads to a loss of one *N*-linked glycan because of disruption of the generic *N*-glycosylation signal. This loss of a carbohydrate is not accompanied by significant structural changes (Fig. 3). Together with the profound deficiency of T14 to sequester MICA/B, this suggests that this carbohydrate may mediate an essential direct contact with corresponding carbohydrates of the heavily glycosylated MICA/B proteins. Consistent with this disparate phenotype, carbohydrates are not required for interaction with HLA-I (40, 55). It will be interesting to investigate the role of carbohydrates for MICA/B interaction in greater detail. Some mutants such as P9, I37, G55, Y60, V62, and V64 show a similar effect on both target proteins (Fig. 8, light gray shading). This is reminiscent of the phenotype of the cysteine mutants C11, C22, C28, and C83 that essentially abrogated both HLA-I and MICA/B downregulation (15). For most other mutants, however, the retention of MICA/B was less severely affected than that of HLA-I. Prominent examples are W52, M87, W96, and P97 in which HLA-I downregulation was essentially abrogated, whereas a significant proportion of MICA/B was retained (Fig. 8, black shading). For K27 and K42, the mutation-induced effect on HLA expression, although relatively small, is also 2.3-fold higher than that seen for MICA/B. An obvious explanation would be that E3/19K has a higher affinity to MICA/B as compared with HLA-I. Although a higher affinity interaction in the absence of β_2-m may be plausible the failure to detect MICA/B-E3/19K complexes in detergent lysates argues against this possibility. Therefore, we suggest that these amino acids are preferentially involved in the downregulation and binding of HLA-I and are less important for MICA/B downregulation.

The availability of four conformation-sensitive mAbs allowed us to relate functional activities of the E3/19K mutants to structural alterations induced by the mutations. Based on secondary structure prediction, the luminal domain comprises a relatively "variable" core domain (aa 1–78) composed of six β-strands connected by loop regions that may be bound by mAbs [Fig. 8 and (57)]. This is followed by a more "conserved domain" between aa 79–98 of Ad2 E3/19K (56, 72) adjacent to the transmembrane segment (see also Fig. 1) that is predicted to contain a 13–15-aa-long α-helix (Fig. 8, cylinder) that is followed C-terminally by a block of conserved amino acids, W96, P97, and P98 that may represent a β turn-like element. With the exception of P9, mutants in the *N*-terminal part (i.e., E5, T14, K27, and K42) show only minimal or minor structural changes as evidenced by the unaltered binding pattern of Tw1.3 and 3F4, and only some minor impact on the 3A9 epitope. This correlates with the minimal, if any, functional alterations observed. For most other mutants in this domain (P9, I37, W52, G55, Y60, V62, and V64), the functional changes are paralleled by considerable structural alterations as evidenced by a 7–20-fold increase of both 3F4 and 10A2 binding (not shown) and a dramatic loss of Tw1.3 binding. However, in each case, the pattern of mAb binding confirms that the disulfide bonds within E3/19K are intact. Thus, amino acids in the three central β-strands appear to be critical for the structural integrity affecting secondary structural entities, whereas mutations in loops 4 and 5 are more benign, largely retaining, for example, the capacity to downregulate MICA/B (K42, W52, and G55).

The "conserved domain" has been proposed to be important for HLA association, possibly by influencing the correct folding of more distal portions of the molecule (56). Surprisingly, the majority of these mutants in this domain (F79, M82, D84, L95, and P98) did neither exhibit major structural alterations nor deficiencies in coimmunoprecipitation of HLA-I (Fig. 2). In stark contrast, M87 and W96 nearly completely lost the ability to form complexes with HLA-I, and accordingly were essentially unable to retain HLA-I intracellularly. The particular importance of M87 is supported by previous observations by Flomenberg et al. (56) in which the equivalent residue M110 of the Ad35 E3/19K protein was mutated to lysine, resulting in a loss of binding to monkey MHC-I molecules. Thus, we conclude that M87 plays a crucial functional role in several E3/19K molecules and the loss of function is unrelated to the charge alteration. Most importantly, the minimal alterations in mAb binding (57) suggest that the mutation does not induce major conformational changes, indicating that M87 may be directly involved in HLA-I binding. Interestingly, in species D Ads methionine is replaced by leucine. Therefore, it will be interesting to see whether species D has a similar targeting profile for HLA-I and MICA/B as species C (55). Similarly, a greatly reduced ability to form complexes with HLA-I associated with a lack of HLA-I downregulation was seen for the W96 mutant. Again, we did not find evidence for major structural alterations when monitoring the epitopes of Tw1.3, 3A9, 3F4, and 10A2 (Fig. 3, and data not shown). Thus, W96 can also be considered part of the interface interacting with HLA-I. Interestingly, the effect of the W96A mutation on MICA/B downregulation was relatively benign as was that of the neighboring aa P97, lending further support that the structural changes are rather subtle and locally restricted. It is speculated that the WPP motif may influence the angle of the E3/19K luminal domain. The substitution of alanine for aspartic acid in position 84 had only a minor effect on HLA-I complex formation, which contrasts with the data by Flomenberg et al. (56) who observed an 80% reduction of coprecipitation when D84 was replaced by glycine in Ad35. This difference might be explained by the different nature of the

substituted amino acid, with glycine being less favored than alanine in α helices, and the different properties of monkey versus human MHC-I molecules.

Contrasting with the SNAP analysis that predicted that most mutations in the conserved domain will result in nonneutral functional changes (Fig. 7*B*), it appears that with the exception of M87 and W96 alterations in the conserved domain had little impact on HLA-I–binding activity. It will be interesting to see whether these amino acids are of particular relevance for MICA/B downregulation or for interaction with as yet unknown target molecules. Overall, it is very unusual for a protein to have predicted such a large number of functionally important residues. However, transmembrane proteins generally have significantly more constraints on sequence than globular molecules because of the structural limitations imposed by membrane localization. Nevertheless, it would be prudent to further experimentally validate SNAP predictions (both neutral and nonneutral) in an effort to identify functionally important sites in E3/19K.

Many viruses evolved mechanisms to downregulate MHC-I to evade cytotoxic CD8 T cells (25, 67). As this viral activity may make such cells more susceptible to NK cells, many viruses express in addition immunoevasins that target NK cells (26, 27). Multiple strategies are used, a very common one is to suppress the expression of ligands for the major activating NK receptor NKG2D, which is also expressed on CD8 T cells. Human and mouse cytomegalovirus use a whole range of molecules for downregulation of MHC-I and NKG2D ligands (26, 27). By contrast, Ad appears to use solely E3/19K to avoid recognition by both CTL and NK cells (15). In this respect, E3/19K is most similar to m152/gp40 of mouse cytomegalovirus that also targets both MHC-I and NKG2D ligands (27, 73). The involvement of multiple target molecules that interact with receptors on different cell types (NK and CTL) makes it difficult to predict the effect of viral subversion of innate and adaptive cytotoxic lymphocytes. For example, NKG2D may or may not contribute to activation of CD8 T cells (73, 74). Infection with Ads and Ad vectors that lack E3/19K has been shown to provoke NK cell lysis (15, 28, 75). Our data suggest that it might be possible to design Ads that may only affect one E3/19K target molecule, MICA/B or MHC-I. In this way, it may be possible to dissect the rather complex interactions between Ads and NK cells and other NKGD-bearing lymphocytes. This knowledge should be very useful for optimization of Ad vectors, including replication-competent oncolytic Ad vectors.

Acknowledgments

We thank Dr. E. Oliver-Jones (University of Warwick) for critically reading the manuscript and the helpful comments. We are indebted to Burkhard Rost for his helpful insight in development of SNAP.

Disclosures

The authors have no financial conflicts of interest.

References

1. Wold, W. S. M., and M. S. Horwitz. 2007. Adenoviruses. In *Fields Virology*, 5th Ed. , Knipe, D. M., P. M. Howley, D. E. Griffin, and R. A. Lamb, eds. Lippincott Williams & Wilkins, Philadelphia, p. 2395–2436.
2. Berk, A. J. 2007. Adenoviridae: The viruses and their replication. In *Fields Virology*, 5th Ed. , Knipe, D. M., P. M. Howley, D. E. Griffin, and R. A. Lamb, eds. Lippincott Williams & Wilkins, Philadelphia, p. 2355–2394.
3. Fox, J. P., C. E. Hall, and M. K. Cooney. 1977. The Seattle Virus Watch. VII. Observations of adenovirus infections. *Am. J. Epidemiol.* 105: 362–386.
4. Garnett, C. T., G. Talekar, J. A. Mahr, W. Huang, Y. Zhang, D. A. Ornelles, and L. R. Gooding. 2009. Latent species C adenoviruses in human tonsil tissues. *J. Virol.* 83: 2417–2428.
5. Burgert, H.-G., Z. Ruzsics, S. Obermeier, A. Hilgendorf, M. Windheim, and A. Elsing. 2002. Subversion of host defense mechanisms by adenoviruses. *Curr. Top. Microbiol. Immunol.* 269: 273–318.
6. Russell, W. C. 2009. Adenoviruses: update on structure and function. *J. Gen. Virol.* 90: 1–20.
7. Windheim, M., A. Hilgendorf, and H.-G. Burgert. 2004. Immune evasion by adenovirus E3 proteins: exploitation of intracellular trafficking pathways. *Curr. Top. Microbiol. Immunol.* 273: 29–85.
8. Lichtenstein, D. L., K. Toth, K. Doronin, A. E. Tollefson, and W. S. Wold. 2004. Functions and mechanisms of action of the adenovirus E3 proteins. *Int. Rev. Immunol.* 23: 75–111.
9. McNees, A. L., and L. R. Gooding. 2002. Adenoviral inhibitors of apoptotic cell death. *Virus Res.* 88: 87–101.
10. Burgert, H.-G., and J. H. Blusch. 2000. Immunomodulatory functions encoded by the E3 transcription unit of adenoviruses. *Virus Genes* 21: 13–25.
11. Bruder, J. T., T. Jie, D. L. McVey, and I. Kovesdi. 1997. Expression of gp19K increases the persistence of transgene expression from an adenovirus vector in the mouse lung and liver. *J. Virol.* 71: 7623–7628.
12. Ginsberg, H. S., U. Lundholm-Beauchamp, R. L. Horswood, B. Pernis, W. S. Wold, R. M. Chanock, and G. A. Prince. 1989. Role of early region 3 (E3) in pathogenesis of adenovirus disease. *Proc. Natl. Acad. Sci. U.S.A.* 86: 3823–3827.
13. von Herrath, M. G., S. Efrat, M. B. Oldstone, and M. S. Horwitz. 1997. Expression of adenoviral E3 transgenes in β cells prevents autoimmune diabetes. *Proc. Natl. Acad. Sci. U.S.A.* 94: 9808–9813.
14. Burgert, H.-G. 1996. Subversion of the MHC class I antigen-presentation pathway by adenoviruses and herpes simplex viruses. *Trends Microbiol.* 4: 107–112.
15. McSharry, B. P., H.-G. Burgert, D. P. Owen, R. J. Stanton, V. Prod'homme, M. Sester, K. Koebernick, V. Groh, T. Spies, S. Cox, et al. 2008. Adenovirus E3/19K promotes evasion of NK cell recognition by intracellular sequestration of the NKG2D ligands major histocompatibility complex class I chain-related proteins A and B. *J. Virol.* 82: 4585–4594.
16. Elsing, A., and H.-G. Burgert. 1998. The adenovirus E3/10.4K-14.5K proteins down-modulate the apoptosis receptor Fas/Apo-1 by inducing its internalization. *Proc. Natl. Acad. Sci. U.S.A.* 95: 10072–10077.
17. Schneider-Brachert, W., V. Tchikov, O. Merkel, M. Jakob, C. Hallas, M.-L. Kruse, P. Groitl, A. Lehn, E. Hildt, J. Held-Feindt, et al. 2006. Inhibition of TNF receptor 1 internalization by adenovirus 14.7K as a novel immune escape mechanism. *J. Clin. Invest.* 116: 2901–2913.
18. Fessler, S. P., F. Delgado-Lopez, and M. S. Horwitz. 2004. Mechanisms of E3 modulation of immune and inflammatory responses. *Curr. Top. Microbiol. Immunol.* 273: 113–135.
19. Burgert, H.-G., and S. Kvist. 1985. An adenovirus type 2 glycoprotein blocks cell surface expression of human histocompatibility class I antigens. *Cell* 41: 987–997.
20. Andersson, M., A. McMichael, and P. A. Peterson. 1987. Reduced allorecognition of adenovirus-2 infected cells. *J. Immunol.* 138: 3960–3966.
21. Cox, J. H., J. R. Bennink, and J. W. Yewdell. 1991. Retention of adenovirus E19 glycoprotein in the endoplasmic reticulum is essential to its ability to block antigen presentation. *J. Exp. Med.* 174: 1629–1637.
22. Rawle, F. C., A. E. Tollefson, W. S. Wold, and L. R. Gooding. 1989. Mouse anti-adenovirus cytotoxic T lymphocytes. Inhibition of lysis by E3 gp19K but not E3 14.7K. *J. Immunol.* 143: 2031–2037.
23. Tanaka, Y., and S. S. Tevethia. 1988. Differential effect of adenovirus 2 E3/19K glycoprotein on the expression of H-2Kb and H-2Db class I antigens and H-2Kb- and H-2Db-restricted SV40-specific CTL-mediated lysis. *Virology* 165: 357–366.
24. Burgert, H.-G., J. L. Maryanski, and S. Kvist. 1987. "E3/19K" protein of adenovirus type 2 inhibits lysis of cytolytic T lymphocytes by blocking cell-surface expression of histocompatibility class I antigens. *Proc. Natl. Acad. Sci. U.S.A.* 84: 1356–1360.
25. Hansen, T. H., and M. Bouvier. 2009. MHC class I antigen presentation: learning from viral evasion strategies. *Nat. Rev. Immunol.* 9: 503–513.
26. Lodoen, M. B., and L. L. Lanier. 2005. Viral modulation of NK cell immunity. *Nat. Rev. Microbiol.* 3: 59–69.
27. Jonjić, S., M. Babić, B. Polić, and A. Krmpotić. 2008. Immune evasion of natural killer cells by viruses. *Curr. Opin. Immunol.* 20: 30–38.
28. Tomasec, P., E. C. Wang, V. Groh, T. Spies, B. P. McSharry, R. J. Aicheler, R. J. Stanton, and G. W. Wilkinson. 2007. Adenovirus vector delivery stimulates natural killer cell recognition. *J. Gen. Virol.* 88: 1103–1108.
29. Andersson, M., S. Pääbo, T. Nilsson, and P. A. Peterson. 1985. Impaired intracellular transport of class I MHC antigens as a possible means for adenoviruses to evade immune surveillance. *Cell* 43: 215–222.
30. Sester, M., and H.-G. Burgert. 1994. Conserved cysteine residues within the E3/19K protein of adenovirus type 2 are essential for binding to major histocompatibility complex antigens. *J. Virol.* 68: 5423–5432.
31. Nilsson, T., M. Jackson, and P. A. Peterson. 1989. Short cytoplasmic sequences serve as retention signals for transmembrane proteins in the endoplasmic reticulum. *Cell* 58: 707–718.
32. Jackson, M. R., T. Nilsson, and P. A. Peterson. 1990. Identification of a consensus motif for retention of transmembrane proteins in the endoplasmic reticulum. *EMBO J.* 9: 3153–3162.
33. Jackson, M. R., T. Nilsson, and P. A. Peterson. 1993. Retrieval of transmembrane proteins to the endoplasmic reticulum. *J. Cell Biol.* 121: 317–333.
34. Gabathuler, R., and S. Kvist. 1990. The endoplasmic reticulum retention signal of the E3/19K protein of adenovirus type 2 consists of three separate amino acid segments at the carboxy terminus. *J. Cell Biol.* 111: 1803–1810.
35. Teasdale, R. D., and M. R. Jackson. 1996. Signal-mediated sorting of membrane proteins between the endoplasmic reticulum and the golgi apparatus. *Annu. Rev. Cell Dev. Biol.* 12: 27–54.

36. Bennett, E. M., J. R. Bennink, J. W. Yewdell, and F. M. Brodsky. 1999. Cutting edge: adenovirus E19 has two mechanisms for affecting class I MHC expression. *J. Immunol.* 162: 5049–5052.
37. Sester, M., D. Feuerbach, R. Frank, T. Preckel, A. Gutermann, and H.-G. Burgert. 2000. The amyloid precursor-like protein 2 associates with the major histocompatibility complex class I molecule K(d). *J. Biol. Chem.* 275: 3645–3654.
38. Liu, H., W. F. Stafford, and M. Bouvier. 2005. The endoplasmic reticulum lumenal domain of the adenovirus type 2 E3-19K protein binds to peptide-filled and peptide-deficient HLA-A*1101 molecules. *J. Virol.* 79: 13317–13325.
39. Morris, C. R., J. L. Petersen, S. E. Vargas, H. R. Turnquist, M. M. McIlhaney, S. D. Sanderson, J. T. Bruder, Y. Y. L. Yu, H.-G. Burgert, and J. C. Solheim. 2003. The amyloid precursor-like protein 2 and the adenoviral E3/19K protein both bind to a conformational site on H-2Kd and regulate H-2Kd expression. *J. Biol. Chem.* 278: 12618–12623.
40. Burgert, H.-G., and S. Kvist. 1987. The E3/19K protein of adenovirus type 2 binds to the domains of histocompatibility antigens required for CTL recognition. *EMBO J.* 6: 2019–2026.
41. Beier, D. C., J. H. Cox, D. R. Vining, P. Cresswell, and V. H. Engelhard. 1994. Association of human class I MHC alleles with the adenovirus E3/19K protein. *J. Immunol.* 152: 3862–3872.
42. Feuerbach, D., S. Etteldorf, C. Ebenau-Jehle, J. P. Abastado, D. Madden, and H.-G. Burgert. 1994. Identification of amino acids within the MHC molecule important for the interaction with the adenovirus protein E3/19K. *J. Immunol.* 153: 1626–1636.
43. Jefferies, W. A., and H.-G. Burgert. 1990. E3/19K from adenovirus 2 is an immunosubversive protein that binds to a structural motif regulating the intracellular transport of major histocompatibility complex class I proteins. *J. Exp. Med.* 172: 1653–1664.
44. Liu, H., J. Fu, and M. Bouvier. 2007. Allele- and locus-specific recognition of class I MHC molecules by the immunomodulatory E3-19K protein from adenovirus. *J. Immunol.* 178: 4567–4575.
45. Flomenberg, P., E. Gutierrez, and K. T. Hogan. 1994. Identification of class I MHC regions which bind to the adenovirus E3-19k protein. *Mol. Immunol.* 31: 1277–1284.
46. Körner, H., and H. G. Burgert. 1994. Down-regulation of HLA antigens by the adenovirus type 2 E3/19K protein in a T-lymphoma cell line. *J. Virol.* 68: 1442–1448.
47. Cox, J. H., J. W. Yewdell, L. C. Eisenlohr, P. R. Johnson, and J. R. Bennink. 1990. Antigen presentation requires transport of MHC class I molecules from the endoplasmic reticulum. *Science* 247: 715–718.
48. Kvist, S., L. Östberg, H. Persson, L. Philipson, and P. A. Peterson. 1978. Molecular association between transplantation antigens and cell surface antigen in adenovirus-transformed cell line. *Proc. Natl. Acad. Sci. U.S.A.* 75: 5674–5678.
49. Lévy, F., and S. Kvist. 1990. Co-expression of the human HLA-B27 class I antigen and the E3/19K protein of adenovirus-2 in insect cells using a baculovirus vector. *Int. Immunol.* 2: 995–1002.
50. Pääbo, S., B. M. Bhat, W. S. Wold, and P. A. Peterson. 1987. A short sequence in the COOH-terminus makes an adenovirus membrane glycoprotein a resident of the endoplasmic reticulum. *Cell* 50: 311–317.
51. Pääbo, S., F. Weber, T. Nilsson, W. Schaffner, and P. A. Peterson. 1986. Structural and functional dissection of an MHC class I antigen-binding adenovirus glycoprotein. *EMBO J.* 5: 1921–1927.
52. Gabathuler, R., F. Lévy, and S. Kvist. 1990. Requirements for the association of adenovirus type 2 E3/19K wild-type and mutant proteins with HLA antigens. *J. Virol.* 64: 3679–3685.
53. Hermiston, T. W., R. A. Tripp, T. Sparer, L. R. Gooding, and W. S. Wold. 1993. Deletion mutation analysis of the adenovirus type 2 E3-gp19K protein: identification of sequences within the endoplasmic reticulum lumenal domain that are required for class I antigen binding and protection from adenovirus-specific cytotoxic T lymphocytes. *J. Virol.* 67: 5289–5298.
54. Pääbo, S., T. Nilsson, and P. A. Peterson. 1986. Adenoviruses of subgenera B, C, D, and E modulate cell-surface expression of major histocompatibility complex class I antigens. *Proc. Natl. Acad. Sci. U.S.A.* 83: 9665–9669.
55. Deryckere, F., and H.-G. Burgert. 1996. Early region 3 of adenovirus type 19 (subgroup D) encodes an HLA-binding protein distinct from that of subgroups B and C. *J. Virol.* 70: 2832–2841.
56. Flomenberg, P., J. Szmulewicz, E. Gutierrez, and H. Lupatkin. 1992. Role of the adenovirus E3-19k conserved region in binding major histocompatibility complex class I molecules. *J. Virol.* 66: 4778–4783.
57. Menz, B., M. Sester, K. Koebernick, R. Schmid, and H.-G. Burgert. 2008. Structural analysis of the adenovirus type 2 E3/19K protein using mutagenesis and a panel of conformation-sensitive monoclonal antibodies. *Mol. Immunol.* 46: 16–26.
58. Bromberg, Y., G. Yachdav, and B. Rost. 2008. SNAP predicts effect of mutations on protein function. *Bioinformatics* 24: 2397–2398.
59. Bromberg, Y., and B. Rost. 2007. SNAP: predict effect of non-synonymous polymorphisms on function. *Nucleic Acids Res.* 35: 3823–3835.
60. Körner, H., U. Fritzsche, and H.-G. Burgert. 1992. Tumor necrosis factor α stimulates expression of adenovirus early region 3 proteins: implications for viral persistence. *Proc. Natl. Acad. Sci. U.S.A.* 89: 11857–11861.
61. Wold, W. S. M., A. E. Tollefson, and T. W. Hermiston. 1995. E3 transcription unit of adenovirus. *Curr. Top. Microbiol. Immunol.* 199/I: 237–274.
62. Hilgendorf, A., J. Lindberg, Z. Ruzsics, S. Höning, A. Elsing, M. Löfqvist, H. Engelmann, and H.-G. Burgert. 2003. Two distinct transport motifs in the adenovirus E3/10.4-14.5 proteins act in concert to down-modulate apoptosis receptors and the epidermal growth factor receptor. *J. Biol. Chem.* 278: 51872–51884.
63. Parham, P., and F. M. Brodsky. 1981. Partial purification and some properties of BB7.2. A cytotoxic monoclonal antibody with specificity for HLA-A2 and a variant of HLA-A28. *Hum. Immunol.* 3: 277–299.
64. Groh, V., R. Rhinehart, H. Secrist, S. Bauer, K. H. Grabstein, and T. Spies. 1999. Broad tumor-associated expression and recognition by tumor-derived gamma delta T cells of MICA and MICB. *Proc. Natl. Acad. Sci. U.S.A.* 96: 6879–6884.
65. Welte, S. A., C. Sinzger, S. Z. Lutz, H. Singh-Jasuja, K. L. Sampaio, U. Eknigk, H. G. Rammensee, and A. Steinle. 2003. Selective intracellular retention of virally induced NKG2D ligands by the human cytomegalovirus UL16 glycoprotein. *Eur. J. Immunol.* 33: 194–203.
66. Bromberg, Y., J. Overton, C. Vaisse, R. L. Leibel, and B. Rost. 2009. In silico mutagenesis: a case study of the melanocortin 4 receptor. *FASEB J.* 23: 3059–3069.
67. Røder, G., L. Geironson, I. Bressendorff, and K. Paulsson. 2008. Viral proteins interfering with antigen presentation target the major histocompatibility complex class I peptide-loading complex. *J. Virol.* 82: 8246–8252.
68. Severinsson, L., I. Martens, and P. A. Peterson. 1986. Differential association between two human MHC class I antigens and an adenoviral glycoprotein. *J. Immunol.* 137: 1003–1009.
69. Feuerbach, D., and H. G. Burgert. 1993. Novel proteins associated with MHC class I antigens in cells expressing the adenovirus protein E3/19K. *EMBO J.* 12: 3153–3161.
70. Tuli, A., M. Sharma, M. M. McIlhaney, J. E. Talmadge, N. Naslavsky, S. Caplan, and J. C. Solheim. 2008. Amyloid precursor-like protein 2 increases the endocytosis, instability, and turnover of the H2-K(d) MHC class I molecule. *J. Immunol.* 181: 1978–1987.
71. Tuli, A., M. Sharma, X. Wang, L. C. Simone, H. L. Capek, S. Cate, W. H. Hildebrand, N. Naslavsky, S. Caplan, and J. C. Solheim. 2009. Amyloid precursor-like protein 2 association with HLA class I molecules. *Cancer Immunol. Immunother.* 58: 1419–1431.
72. Flomenberg, P. R., M. Chen, and M. S. Horwitz. 1988. Sequence and genetic organization of adenovirus type 35 early region 3. *J. Virol.* 62: 4431–4437.
73. Pinto, A. K., A. M. Jamieson, D. H. Raulet, and A. B. Hill. 2007. The role of NKG2D signaling in inhibition of cytotoxic T-lymphocyte lysis by the Murine cytomegalovirus immunoevasin m152/gp40. *J. Virol.* 81: 12564–12571.
74. Groh, V., R. Rhinehart, J. Randolph-Habecker, M. S. Topp, S. R. Riddell, and T. Spies. 2001. Costimulation of CD8alphabeta T cells by NKG2D via engagement by MIC induced on virus-infected cells. *Nat. Immunol.* 2: 255–260.
75. Routes, J. M., S. Ryan, K. Morris, R. Takaki, A. Cerwenka, and L. L. Lanier. 2005. Adenovirus serotype 5 E1A sensitizes tumor cells to NKG2D-dependent NK cell lysis and tumor rejection. *J. Exp. Med.* 202: 1477–1482.